Journal of Materials Chemistry C

ROYAL SOCIETY OF CHEMISTRY

PAPER

View Article Online
View Journal | View Issue

Cite this: J. Mater. Chem. C, 2024, 12, 4261

Poly(3,4-ethylenedioxythiophene)/poly(bis(4-phenoxysulfonic acid)phosphazene) conductive composites: an alternative interfacial layer to PEDOT : PSS†

Elif Büşra Çelebi, [ab] Joseph Cameron, [b] Peter J. Skabara [b] and Ferda Hacıvelioğlu *[ab]

Received 9th January 2024,
Accepted 25th February 2024

DOI: 10.1039/d4tc00109e

rsc.li/materials-c

Poly(3,4-ethylenedioxythiophene):poly(styrene sulfonate) (PEDOT : PSS) is a popular solution-processable hole transporting layer used in organic semiconductor devices such as organic light-emitting diodes or organic photovoltaics. It has benefits such as suitability for orthogonal processing, tunable conductivity and smooth film formation, yet the PSS polyelectrolyte is prone to degradation, impacting device performance or lifetime. In this work we present the use of PEDOT blends with a poly(bis(4-phenoxysulfonic acid)phosphazene) (PSAP) polyelectrolyte and study the effect of the PEDOT : PSAP ratio on the composite material properties. A comparable doping level can be achieved in PEDOT : PSAP films with respect to PEDOT : PSS and, as a result, an appropriate electrical conductivity for use as a hole transport layer can be achieved. Finally, when applied in organic light-emitting diodes, the use of PEDOT : PSAP hole transport layers can boost the external quantum efficiency, highlighting the promising performance of PSAP polyelectrolyte in conductive blends.

Introduction

Among the family of conjugated conducting polymers, poly(3,4-ethylenedioxythiophene) (PEDOT) is one of the most studied due to its unique properties such as high transparency in the visible region, high environmental stability, and tunable conductivity.[1] Although it was initially designed as a solution-processable material, it was found to be insoluble in water or common organic solvents. PEDOT's solution processability problem could be overcome by the incorporation of the water-soluble polyanionic charge balancer poly(styrene sulfonic acid) (PSS) which allows the dispersion of the whole macromolecular salt system (PEDOT : PSS) in water.[2] Since solution processability was achieved, PEDOT : PSS has become a prominent material for a number of applications including organic electrodes,[3] batteries[4] and supercapacitors,[5] and artificial muscle applications.[6] However, the acidic and hygroscopic nature of PSS itself brought some unwanted properties to the final conducting material.[7] For example, if PEDOT : PSS is used between a transparent conducting electrode, usually indium-doped tin oxide (ITO), and the active layer in an OLED, PSS etches the ITO which results in migration of indium and tin to the inner layers.[8,9] This results in the degradation of the device and shortened device lifetime, which is an issue that must be overcome to compete with inorganic semiconductor-based technologies. In addition to its hygroscopicity and acidity, PSS is prone to degradation in the presence of radicals,[10–12] or oxidants,[13] while PEDOT is usually synthesised inside an aqueous solution of PSS in the presence of very strong oxidants such as ammonium persulfate[14] or sodium persulfate.[15,16] Therefore, a polymer backbone with a high oxidative stability is highly sought to cope with the instability problems. In contrast to styrene-based polymers, poly(aryloxyphosphazenes) are viable alternatives with some unique properties.[17] Poly(phosphazenes) have alternating P and N atoms on the main chain which are in their highest oxidation state and thus the poly(phosphazene) backbone is highly resistant to thermal and chemical oxidative conditions.[17] Whilst poly(dichlorophosphazene) is unstable in a moist environment, it is an effective precursor for lots of different and highly stable poly(phosphazenes) by the macromolecular nucleophilic substitution of the chlorine atoms by alcohols, phenols, or nucleophilic amines in the presence of a base. Although it is typically challenging to synthesise sulfonic acid functionalised poly(aryloxyphosphazenes), some of us recently introduced a simple synthetic procedure for the preparation of fully or partially sulfonated poly(aryloxyphosphazenes) by covalent protection of the sulfonic acid moiety.[18] This progress then led us to develop single-component water-soluble PEDOT-grafted sulfonic acid functionalised

[a] Gebze Technical University Department of Chemistry, Gebze, Kocaeli, 41400, Turkey. E-mail: ferda.hacivelioglu@glasgow.ac.uk, peter.skabara@glasgow.ac.uk
[b] University of Glasgow, School of Chemistry, G12 8QQ, Glasgow, UK

† Electronic supplementary information (ESI) available. See DOI: https://doi.org/10.1039/d4tc00109e

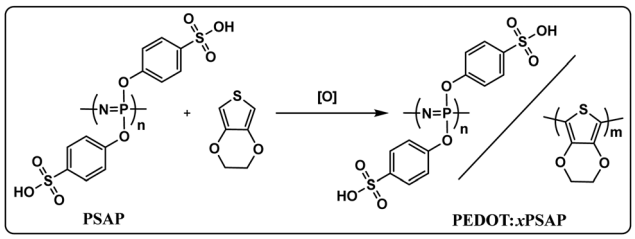

Scheme 1 Synthetic pathway to PEDOT : *x*PSAP.

poly(aryloxyphosphazene) copolymers.[19] However, growing PEDOT graft arms on another polymer requires a specially designed precursor which has thiophene anchors on its backbone, therefore it is not as simple to polymerise as EDOT in the presence of poly(bis(4-oxybenzene sulfonic acid)phosphazene), *i.e.*, PSAP, which is the polyphosphazene analogue of the PSS.

In this study, we prepared a series of PEDOT : *x*PSAP composites by varying the EDOT feed ratio into aqueous solutions of PSAP which were then chemically oxidised to PEDOT by using a fixed oxidant-to-monomer ratio ($(NH_4)_2S_2O_8$, APS / EDOT of 6 : 5). Towards the application of PSAP in optoelectronic devices, we synthesised the poly(dichlorophosphazene) by living cationic polymerisation of the monomer $Cl_3P{=}NSiMe_3$, which leads to low dispersity ($Đ$) and controlled molecular weight (M_w) poly(phosphazenes), followed by functionalisation with 4-oxybenzene sulfonic acid.[20] The resulting composites were then tested as an alternative hole transport layer (HTL) to PEDOT : PSS (Al 4083) on Super Yellow (SY)-based OLED devices with a configuration of indium-doped tin oxide (ITO)/HTL/SY/Ca/Al.

Results and discussion

The preparation of PEDOT : *x*PSAP macromolecular salt systems were very similar to the preparation of PEDOT : PSS, as depicted in Scheme 1. In this study the precursor, poly(dichlorophosphazene) (PDCP), was synthesised from the living cationic polymerisation of $Cl_3P{=}NSiMe_3$ as it gives quantitative conversion and an almost monodisperse polymer with a controlled molecular weight.[21] The PDCP synthesised by this route had a M_w of 2.05 × 10^5 Da and $Đ$ = 1.25 with a monomer-to-initiator (PCl_5) ratio of 400/1, which was very similar to the literature value as determined by gel permeation chromatography or size exclusion chromatography measurements. Then, PDCP was successfully derivatised to poly(bis(4-oxybenzene sulfonic acid) phosphazene) (PSAP) in a two-step process: first, a nucleophilic substitution reaction of PDCP with ethyl 4-hydroxybenzene sulfonate in the presence of NaH and then conversion to sulfonic acid by treatment with dilute H_2SO_4.[18] After purification of the PSAP by a few ethanol precipitations, a 2% (w/w) stock water solution was used for the chemical oxidative polymerisation of EDOT to PEDOT in the presence of ammonium peroxydisulfate (APS, $(NH_4)_2S_2O_8$). The EDOT feed ratio (w/w) was varied between 1 : 1 to 1 : 11 in odd-number intervals, whilst keeping the EDOT:APS stoichiometric ratio fixed as 1 : 1.2, to optimise the conductivity, optical, and morphological properties of the resulting PEDOT : *x*PSAP composites.

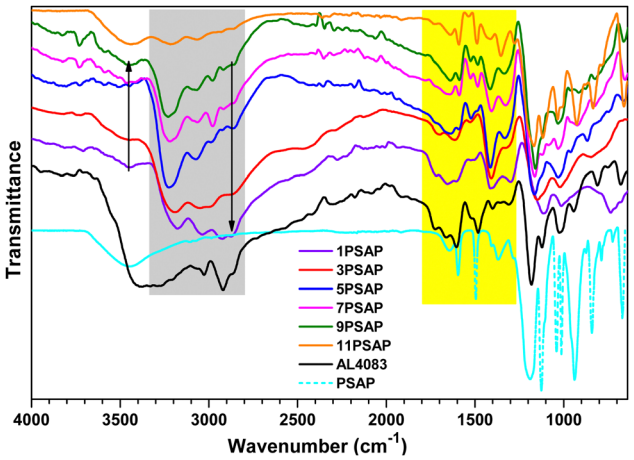

Fig. 1 Solid state(film) FTIR spectra of PSAP, PEDOT : PSS and PEDOT : *x*PSAP samples.

The PEDOT : *x*PSAP blends prepared using different EDOT feed ratios were studied using Fourier-transform infrared (FTIR) spectroscopy, as shown in Fig. 1. PSAP itself has characteristic vibration peaks of –OH, –CH and C=C stretching at 3460, 3100, and 1595 and 1493 cm^{-1}, respectively. The strong vibration peaks at 1360 and 1042 cm^{-1}, and 1122 cm^{-1} can be attributed respectively to S=O (symmetrical, and asymmetrical) and S–O stretching, whilst antisymmetric P–O stretching is observed at 934 cm^{-1}. The spectrum of commercial PEDOT : PSS (Al 4083) has peaks at very similar frequencies with additional PEDOT aliphatic C–H stretching peaks at 2860 and 2915 cm^{-1}, and C–S stretching peaks at 937, 808 and 675 cm^{-1} (Fig. 1). A prominent change in the spectra of the PEDOT : *x*PSAP composites can be seen between 2750 to 3365 cm^{-1}. The –OH stretching moved to 3220 cm^{-1}, which is an indication of intermolecular bonding between PSAP and PEDOT. Furthermore, the remaining free –OH stretching peak at 3460 cm^{-1} increases with the decreasing PEDOT ratio (Fig. 1). Since PSAP has no aliphatic groups and thus no aliphatic –CH stretching, the peaks between 2760 to 2890 cm^{-1} can be assigned to aliphatic –CH vibrations of PEDOT. The relative intensity of this peak increases with increasing amount of PEDOT in the PEDOT : *x*PSAP blends. Another apparent difference in the FTIR spectra of PEDOT : PSS and PEDOT : *x*PSAP compared to PSAP is found in the range between 1660 and 1306 cm^{-1}. The two distinct bands at ~1650 and 1404 cm^{-1}, which have increased intensity with increasing PEDOT ratio in the PEDOT : *x*PSAP composites, can be attributed to the C=C and C–C stretching of PEDOT, also observed in the spectrum of commercial PEDOT : PSS (Al 4083).

The interaction of PEDOT with PSAP in PEDOT : *x*PSAPs was further investigated by UV-Vis absorption measurements (Fig. 2). The poly(phosphazene) backbone does not have absorption in the UV-Vis and NIR range and therefore its fully sulfonated benzene sulfonic acid derivative PSAP will not affect the optical properties of PEDOT. Fig. 2 shows a strong absorption band at 800 nm arising from the polaron transitions of PEDOT for all the materials. The absorption intensity increases

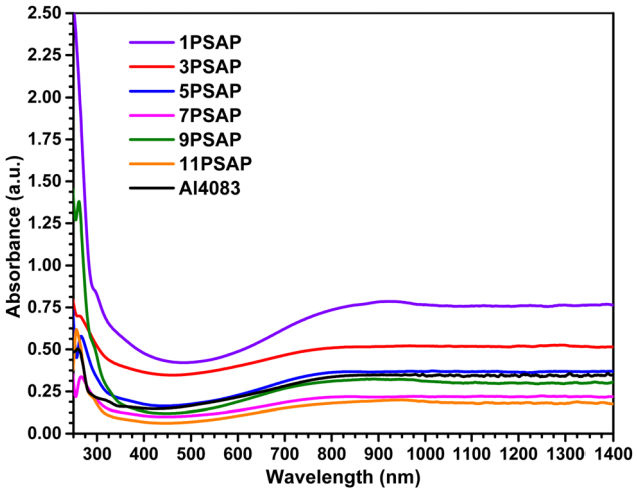

Fig. 2 Comparative UV-Vis spectra of PEDOT : *x*PSAP and PEDOT : PSS (Al4083) samples in 0.2% water.

by the increasing PEDOT ratio in PEDOT : *x*PSAPs. PEDOT : PSS, AL4083 grade, has a PEDOT-to-PSS ratio of 1 : 6 (w/w) and shows very similar absorption behaviour to PEDOT:5PSAP, which has the PEDOT-to-PSAP ratio of 1 : 5 (w/w). This difference is not surprising since PSS has one sulfonic acid per repeating unit of the polymer, whereas PSAP has two sulfonic acid moieties. The PEDOT polaron absorption in the NIR region of the spectra remains almost the same for all materials measured except PEDOT:1PSAP which has an absorption maximum at 925 nm, and then its absorption remains constant up to 1400 nm. Hence, it can be said that all the samples have high polaron concentration ensuring electrical conductivity whilst there is no sign of neutral PEDOT absorption around ~600 nm.

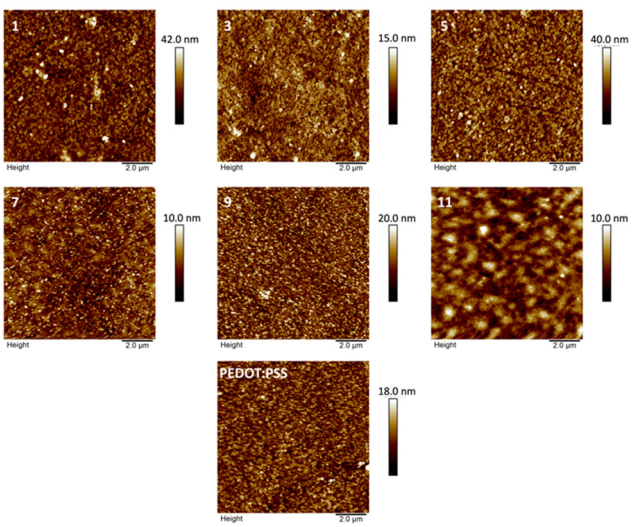

Fig. 3 AFM topography images of PEDOT : *x*PSAP thin films. The root mean square roughness (R_q) for the films were as follows: PEDOT:1PSAP – 5.82 nm; PEDOT:3PSAP – 2.27 nm; PEDOT:5PSAP – 5.90 nm; PEDOT:7PSAP – 1.35 nm; PEDOT:9PSAP – 3.10 nm; PEDOT:11PSAP – 1.50 nm and PEDOT : PSS (Al4083) – 2.64 nm.

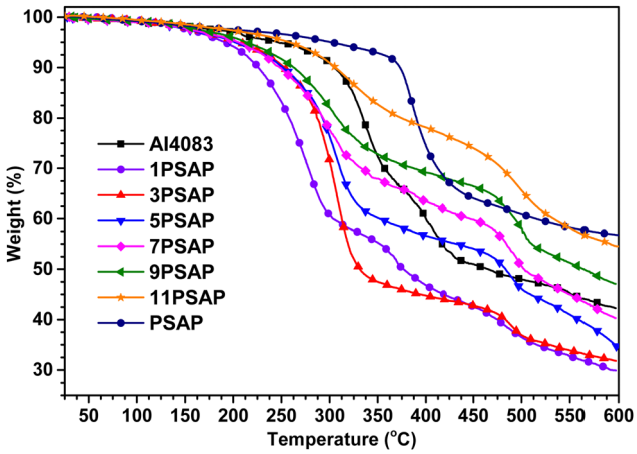

Fig. 4 Comparative TGA results of PSAP, PEDOT : *x*PSAP and PEDOT : PSS.

The similarity between PEDOT : PSS and PEDOT : *x*PSAPs is also evident in the surface morphology as shown from the tapping mode AFM images presented in Fig. 3. The PEDOT:1PSAP film shows some aggregates on the surface which may be caused by an insufficient amount of PSAP to stabilise the PEDOT dispersion in solution. On the other hand, the PEDOT:11PSAP film begins to show potential phase segregation, albeit the height difference between the domains and the bulk remains reasonably small. It can be expected that if the PSAP content were increased there would be further phase segregation. However, in general, the films show good uniformity and as such it can be expected that the PEDOT rich layers are homogenously distributed in the PEDOT : *x*PSAPs, emphasising the good film formation which may arise from the use of poly(aryloxyphosphazenes). The PEDOT : *x*PSAP water dispersions were stable at room temperature without any precipitation over 3 months and only the PEDOT:1PSAP had minor precipitated particles which could be redispersed simply by shaking. Hence, the PEDOT : *x*PSAP water dispersions have similar morphological features to PEDOT : PSS and may be an alternative to PEDOT : PSS for organic electronic device applications.

Thermal stability is another important property of interfacial layers for application in organic electronics which affects the device's lifetime. The TGA plots of the PEDOT : *x*PSAPs are

Table 1 Selected thermal and conductivity data for PEDOT : PSS, PSAP and PEDOT : *x*PSAP

Material	T_d (°C)	% Residue	R_s (Ω □$^{-1}$)	Conductivity (S cm^{-1})
PSAP	373.9	56.8	—	0.04[a]
PEDOT:1PSAP	225.6	29.8	4.9×10^2	2.4×10^{-1}
PEDOT:3PSAP	250.8	31.7	1.1×10^4	1.1×10^{-2}
PEDOT:5PSAP	251.2	34.8	1.0×10^5	1.1×10^{-3}
PEDOT:7PSAP	248.0	40.3	1.1×10^6	1.2×10^{-4}
PEDOT:9PSAP	254.9	46.9	1.2×10^6	1.1×10^{-4}
PEDOT:11PSAP	305.6	54.4	1.2×10^6	9.3×10^{-5}
AL4083	304.6	42.3	1.1×10^6	9.6×10^{-5}

[a] Room temperature ionic conductivity value from ref. 18.

Table 2 Summary of OLED performance with PEDOT : *x*PSAP hole transport layers

HTL	V_{on} (V)	L_{max} (cd m^{-2})	EQE_{max} (%)
PEDOT:**1**PSAP	2.6	28 100	1.40
PEDOT:**3**PSAP	2.6	34 700	1.80
PEDOT:**5**PSAP	2.5	55 300	2.14
PEDOT:**7**PSAP	2.9	17 100	1.82
PEDOT:**9**PSAP	2.5	61 300	2.20
PEDOT:**11**PSAP	2.5	34 500	2.15
AL4083	2.7	65 300	1.81

given in Fig. 4 and the results have been summarised in Table 1. As can be seen from Fig. 4 and Table 1, most of the PEDOT : *x*PSAPs decompose over 250 °C except PEDOT:1PSAP which has the highest PEDOT content. Although it was proven that PSAP and its derivatives have high oxidative and thermal stability,[17] the PEDOT : *x*PSAPs show lower thermal stability compared to PEDOT : PSS (Fig. 4). The decrease of thermal stability with the increase in PEDOT composition, or comparatively lower thermal stability of PEDOT : *x*PSAP at a similar PEDOT content to PEDOT : PSS, is modest and perhaps not particularly significant for most device applications. However, a possible explanation for the lower thermal stability of the PEDOT : *x*PSAPs may be the lack of radical traps in the chemically inert polyphosphazenes which cannot stabilise these species that evolved during the decomposition of PEDOT. Unlike PSAP, *ortho*- positions of the benzene ring of PSS are prone to abstract radicals which subsequently delocalise on to the α-position of the main polymer chain by stabilisation, and then chain scission takes place.[12,13] It is possible that the presence of PEDOT, which already carries the radical polarons, may repair the PSS chain by donating electrons in a process similar to a previously observed cerium-mediated repair of poly(α-methyl styrene sulfonate) analogue.[11] On the other hand, the radical species on the PEDOT may react with the radical carrying α-position of the main PSS chain to form a covalent bond and thus result in a more stable PEDOT adduct. Hence, this may result in a more thermally stable PEDOT : PSS material, and thus explains why the thermal decomposition rate of PEDOT : PSS is lower than PEDOT : *x*PSAPs at a higher (PEDOT:1PSAP and PEDOT:3PSAP) or similar PEDOT content, *i.e.*, PEDOT:5PSAP&PEDOT:7PSAP.

Although PEDOT:1PSAP has lower thermal stability compared to PEDOT : PSS and other analogues in the series, it has an initial conductivity of 0.24 S cm^{-1} similar to high conductivity grade pristine PEDOT : PSS[22] (Table 1). On the other hand, the conductivity decreases to 11 mS cm^{-1} in the PEDOT:3PSAP sample and continues to decrease with a decrease of PEDOT content in PEDOT:5PSAP, PEDOT:7PSAP PEDOT:9PSAP and PEDOT:11PSAP, which have a very similar conductivity to commercial Al4083.

Organic light-emitting diodes were fabricated using the PEDOT : *x*PSAP materials as hole transport layers (HTLs) in place of PEDOT : PSS. The device structure was as follows: ITO/HTL/Super Yellow/Ca/Al. A summary of the device performance achieved using different HTLs is shown in Table 2, while

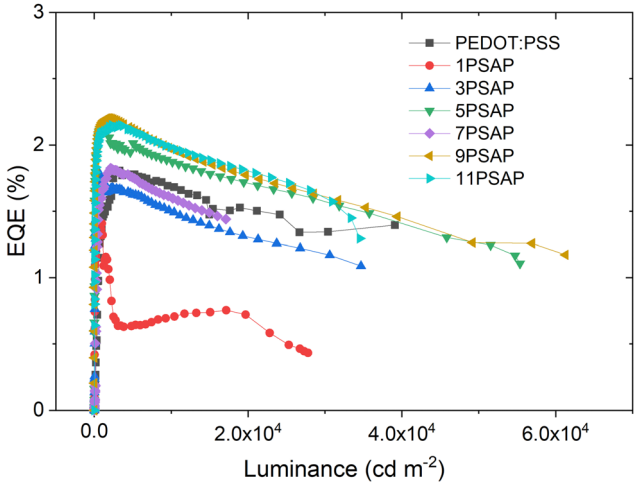

Fig. 5 External quantum efficiency (EQE) *vs.* luminance plots for OLEDs containing PEDOT : PSS or PEDOT : *x*PSAP hole transport layers.

current density–voltage-luminance and external quantum efficiency (EQE) vs luminance plots are shown in Fig. 5 and Fig. S1–S7 (ESI†), respectively.

When the hole transport layer contains PEDOT:1PSAP or PEDOT:3PSAP, the EQE and maximum luminance are lower than observed for the equivalent PEDOT : PSS containing device. However, OLEDs PEDOT:5PSAP, PEDOT:7PSAP, PEDOT:9PSAP and PEDOT:11PSAP all show superior EQEs with respect to the PEDOT : PSS based analogue, although the maximum luminance is greatest in the latter. Optimum performance for OLEDs studying the PEDOT : *x*PSAP series as hole transport layers is achieved in terms of both maximum luminance and EQE for PEDOT:9PSAP. This can be attributed to a combination of factors, with a suitable conductivity ensuring better charge carrier balance in the emissive layer, better thermal stability and smooth surface topography. When the PSAP concentration is increased further, the apparent phase segregation (Fig. 3) begins to limit performance. Overall, we have highlighted how PSAP can be used effectively as a polyelectrolyte for PEDOT blends used as hole transport layers in organic light-emitting diodes.

Conclusion

In this manuscript we have reported the synthesis and application of PEDOT blends with poly(bis(4-phenoxysulfonic acid)-phosphazene) (PSAP) polyelectrolyte. The PEDOT : PSAP films show a high polaron concentration and electrical conductivities comparable to the commercially available PEDOT : PSS blend (Al4083). The composite materials were applied in organic light-emitting diodes as hole transport layers, with devices containing PEDOT:5PSAP, PEDOT:9PSAP and PEDOT:11PSAP giving improved efficiency compared to a PEDOT : PSS-containing analogue. As a result, we have demonstrated that PSAP is a promising polyelectrolyte for use in conductive materials for organic electronics applications.

Experimental

Materials and methods

Ammonium peroxydisulfate (APS) was obtained from Alfa Aesar and 4-hydroxybenzenesulfonic acid hydrate (>85%) was obtained from Tokyo Chemical Industry Co. (TCI) and used without further purification. The deuterated solvents, $CDCl_3$ and D_2O for NMR spectroscopy and the following chemicals were obtained from Merck: NaH (60% suspension in mineral oil), ethanol, H_2SO_4 (98%), tetrahydrofuran (THF), 3,4-ethylenedioxythiophene (EDOT), PCl_5 (98%) and triethyl orthoformate (98%). Super Yellow, poly(1,4-phenylenevinylene) (SY), was obtained from Sigma–Aldrich. PEDOT : PSS (AL4083) was obtained from Ossila Ltd. Deionised (DI) water (18 MΩ) was obtained from a Millipore water purification system. All other reagents and solvents were reagent grade quality and obtained from commercial suppliers.

Equipment

FT-IR spectra of the thin film samples of PEDOT : PSS and PEDOT : *x*PSAPs were recorded on a Jasco FT-IR 4100 spectrometer in attenuated total reflectance (ATR) mode in the range of 4000–650 cm^{-1}. ^1H, ^{13}C, ^{31}P NMR measurements were recorded in $CDCl_3$ and D_2O solutions on a Bruker 500 MHz spectrometer. UV-Vis spectra were recorded on a Shimadzu UV-2600 in the range of 250 to 1400 nm in 0.2% water solutions. Thermal properties of the samples were measured by using Netzsch TG209 F3 *Tarsus* TGA instrument between 25–600 °C at a 20 °C min^{-1} heating rate under constant flow of 30 mL N_2. Atomic force microscopy (AFM) was carried out using a Bruker Innova AFM. DC conductivities of the PEDOT : PSAP thin films were measured by using a Signatone four-point probe with Keithley 2450 source meter. The conductivity of spin-cast PEDOT : *x*PSAP samples were calculated from the following equation,

$$\sigma = \frac{1}{R_s * t}$$

where σ is the conductivity (S cm^{-1}), t is the thickness (cm) of the sample (measured by AFM analysis) (cm), R_s is the sheet resistance (Ω $\square^{-1}$).

Synthesis

Poly(dichlorophosphazene) (PDCP) was synthesised from the room temperature living cationic condensation polymerisation of $Cl_3P{=}NSiMe_3$ with a monomer/initiator (PCl_5) ratio of 400 : 1, according to literature procedure.[21] ^{31}P NMR ($CDCl_3$) δ = −17.5 [br s, –$Cl_2\underline{P}{=}N$–]. GPC/SEC (5% Bu_4NBr, THF mobile phase) $M_w = 2.05 \times 10^5$, PDI = 1.25.

Poly(bis(4-phenoxysulfonic acid)phosphazene) was synthesised by reacting PDCP with ethyl 4-hydroxybenzene sulfonate and subsequent transformation to free acid form according to the literature procedure.[18] ^{31}P NMR (D_2O) δ = −20.5 [br s, 1P, –N = $\underline{P}(OPhSO_3H)_2$]. ^1H NMR (D_2O) δ = 6.5 and 7.1 ppm [two br s, aromatic phenyl protons].

Table 3 Used reagent amounts for the preparation of PEDOT : *x*PSAP composites

Material	EDOT mg	EDOT mmol	APS mg	APS mmol	PSAP/EDOT Ratio (w/w)
PEDOT:**1**PSAP	50.0	0.35	96.3	0.42	**1**
PEDOT:**3**PSAP	16.7	0.12	32.9	0.14	**3**
PEDOT:**5**PSAP	10.0	0.07	19.3	0.08	**5**
PEDOT:**7**PSAP	7.14	0.05	13.8	0.06	**7**
PEDOT:**9**PSAP	5.56	0.04	10.7	0.05	**9**
PEDOT:**11**PSAP	4.55	0.03	8.2	0.04	**11**

Preparation of poly(3,4-ethylenedioxythiophene)/poly(bis(4-phenoxysulfonic acid) phosphazene) (PEDOT : *x*PSAP) water dispersions. Poly(bis(4-phenoxysulfonic acid) phosphazene) (PSAP) (2.0 g, 5.12 mmol) was dissolved in deionised water (100 mL) to obtain a 2% (w/w) stock solution and used for preparation of composites by varying the EDOT feed ratio (n/n). Specific reagent amounts are given in Table 3 and the general experimental procedure was as follows. A 10 mL aliquot of 2% PSAP solution in water was taken from the above stock solution in a round-bottomed 25 mL flask and the corresponding stoichiometric amount of EDOT (Table 3) was added under vigorous stirring. The mixture was stirred for half an hour and the calculated amount of oxidant (APS) in water was added slowly. The reaction turned light blue in 1 hour and was allowed to stir for 2 days. The resulting dark blue mixture was then filtered through a 0.45 μm PTFE syringe filter and labelled as PEDOT : *x*PSAP where *x* denotes the PSAP weight ratio. $\{^1H\}^{31}P$ NMR (D_2O) δ = −20.5 [br s, 1P, $\underline{P}(OPhR)_2$, R = –SO_3H]. ^1H NMR (D_2O) δ = 6.5 and 7.1 ppm [two br s, aromatic phenyl protons], δ = 3.66 ppm [br s, –$OC\underline{H}_2C\underline{H}_2O$–, PEDOT]. ^{13}C NMR (D_2O) δ = 120.1 and 131.9 ppm (disubstituted benzene), 127.3 (br d) and 152.9 ppm (di substituted benzene *ipso* carbons), δ = 115.2 and 141.5 ppm (br s, quaternary C atoms of PEDOT), δ = 62.5, 63.9, 65.4 ppm [br m, –$O\underline{C}H_2\underline{C}H_2O$–, PEDOT].

Device fabrication

OLED devices were fabricated on ITO substrates purchased from Kintec with a sheet resistance of 7 Ω $\square^{-1}$ and ITO thickness of 150 nm. The ITO substrates were cleaned under ultra-sonication using deionised water, acetone, and isopropanol consecutively for 10 minutes. The substrates were dried by blowing compressed air and then treated with oxygen plasma for 10 minutes. The PEDOT : *x*PSAPs and PEDOT : PSS (Heraeus) samples were filtered into 5 mL vials using a 0.45 μm PVDF filter and were spin coated onto the ITO substrates at 3000 rpm for 60 seconds using a Specialty Coating Systems G3P-8 spin coater and the films were annealed at 120 °C for 20 minutes. The films were then transferred to a glove box (MBraun) with controlled oxygen and moisture (O_2 < 0.1 ppm, H_2O < 0.1 ppm). Super Yellow (SY) solution (5 mg mL^{-1}) in anhydrous toluene was prepared a day earlier and kept stirring at 40 °C to ensure complete dissolution of the polymer. Then the SY active layer was spin coated onto the PEDOT : *x*PSAP or

PEDOT:PSS films using a spin coater at 1400 rpm for 60 seconds to obtain a thickness of ~90 nm. 40 nm of Ca (Sigma Aldrich) and 60 nm of Al (Kurt J. Lesker) were respectively deposited by physical vapor deposition at a rate of 0.5 to 1 Å s^{-1}, using an MBRAUN thermal evaporator at pressures of $\sim 10^{-6}$ mbar. The final OLED device structures were glass/ITO/HTL (PEDOT:*x*PSAP or PEDOT:PSS)/SY/Ca/Al and each OLED pixel had an area of 1.5 × 3.5 mm^2. Current–voltage-luminance (IVL) of the devices were measured using a SCS4200 (Keithley) semiconductor characterisation system interfaced with a L203 luminance meter (Irradian).

Data availability

The raw data that supports this manuscript can be found at **http://dx.doi.org/10.5525/gla.researchdata.1540**.

Author contributions

E. B. Ç.: conceptualization, data curation, formal analysis, investigation, writing – original draft. J. C.: data curation, investigation, methodology, writing – original draft. P. J. S.: funding acquisition, project administration, supervision, writing – review & editing. F. H.: Conceptualisation, funding acquisition, project administration, supervision, writing – original draft.

Conflicts of interest

There are no conflicts to declare.

Acknowledgements

We greatly acknowledge the Royal Society for funding our research under the grant number NAF_R2_180625. We also acknowledge TUBITAK for their support for FH (grant number 113Z314) and EBC (2219-International Postdoctoral Research Fellowship). JC thanks the EPSRC for funding (grant number EP/T022477/1).

References

1 Y. Jiang, T. Liu and Y. Zhou, *Adv. Funct. Mater.*, 2020, **30**, 2006213.
2 L. Groenendaal, F. Jonas, D. Freitag, H. Pielartzik and J. R. Reynolds, *Adv. Mater.*, 2000, **12**, 481–494.
3 G. Huseynova, Y. Hyun Kim, J.-H. Lee and J. Lee, *J. Inf. Disp.*, 2020, **21**, 71–91.
4 D. H. Yoon, S. H. Yoon, K.-S. Ryu and Y. J. Park, *Sci. Rep.*, 2016, **6**, 19962.
5 L. Manjakkal, A. Pullanchiyodan, N. Yogeswaran, E. S. Hosseini and R. Dahiya, *Adv. Mater.*, 2020, **32**, 1907254.
6 K. Rohtlaid, G. T. M. Nguyen, S. Ebrahimi-Takalloo, T. N. Nguyen, J. D. W. Madden, F. Vidal and C. Plesse, *Adv. Mater. Technol.*, 2021, **6**, 2001063.
7 J. Cameron and P. J. Skabara, *Mater. Horiz.*, 2020, **7**, 1759–1772.
8 A. Sharma, G. Andersson and D. A. Lewis, *Phys. Chem. Chem. Phys.*, 2011, **13**, 4381–4387.
9 J. Kettle, H. Waters, Z. Ding, M. Horie and G. C. Smith, *Sol. Energy Mater.*, 2015, **141**, 139–147.
10 L. Gubler, S. M. Dockheer and W. H. Koppenol, *J. Electrochem. Soc.*, 2011, **158**, B755.
11 T. M. Nolte, T. Nauser and L. Gubler, *Phys. Chem. Chem. Phys.*, 2020, **22**, 4516–4525.
12 S. M. Dockheer, L. Gubler, P. L. Bounds, A. S. Domazou, G. G. Scherer, A. Wokaun and W. H. Koppenol, *Phys. Chem. Chem. Phys.*, 2010, **12**, 11609–11616.
13 G. Madras and B. J. McCoy, *Chem. Eng. Sci.*, 1997, **52**, 2707–2713.
14 D. A. Ahmad Ruzaidi, M. M. Mahat, Z. Mohamed Sofian, N. A. Nor Hashim, H. Osman, M. A. Nawawi, R. Ramli, K. A. Jantan, M. F. Aizamddin, H. H. Azman, Y. H. Robin Chang and H. H. Hamzah, *Polymers*, 2021, **13**, 2901.
15 S. Ebrahimi, M. Nasiri, S. Agbolaghi, F. Abbasi and R. Sarvari, *J. Polym. Res.*, 2018, **25**, 236.
16 F. Louwet, L. Groenendaal, J. Dhaen, J. Manca, J. Van Luppen, E. Verdonck and L. Leenders, *Synth. Met.*, 2003, **135–136**, 115–117.
17 E. B. Çelebi and F. Hacıvelioğlu, *Polymer*, 2022, **255**, 125175.
18 E. B. Çelebi and F. Hacıvelioğlu, *Polym. Chem.*, 2017, **8**, 3022–3033.
19 E. Büşra Çelebi, N. Demirhan and F. Hacıvelioğlu, *J. Mater. Chem. C*, 2018, **6**, 2672–2677.
20 E. B. Çelebi and F. Hacıvelioğlu, *New J. Chem.*, 2021, **45**, 19364–19372.
21 H. R. Allcock, S. D. Reeves, C. R. de Denus and C. A. Crane, *Macromolecules*, 2001, **34**, 748–754.
22 T. Horii, Y. Li, Y. Mori and H. Okuzaki, *Polym. J.*, 2015, **47**, 695–699.

